IMPROVED ONE DIMENSIONAL ENERGY BALANCE MODELLING UTILISING SKY-VIEW FACTORS DETERMINED FROM DIGITAL IMAGERY

SIRWEC - March 2000: Davos, Switzerland

Lee Chapman
Department of Geography, The University of Birmingham
Birmingham, B15 2TT, UK.

ABSTRACT

The two-way influence of the sky-view factor on the radiation balance results in large variations of road surface temperatures across a road network. A new technique is proposed which enables the direct calculation of the sky-view factor from a digital fish-eye JPEG. The technique is rapid and allows for the influence of the sky-view factor to be studied on a scale not previously possible. The result is that sky-view factors have now been incorporated as a parameter into a 1D EBM which can be used to model road surface temperatures more effectively at both spatial and temporal scales.

INTRODUCTION

Meteorological data collected from Road Weather Stations is processed via a climate model to produce a 24 hour forecast curve for road surface temperature (RST). This curve is then projected around a road network by means of a thermal map. The majority of climate models used in winter road maintenance are loosely based around a 1D energy balance approach, which take into account a vast variety of variables, but rarely the sky-view factor (ψ_s).

ψ_s is a dimensionless parameter represented as a value between zero and one and is a measure of the degree of sky obstruction afforded a location. In perfectly flat and open terrain, ψ_s will approach unity, where as sites with obstructions such as trees and buildings will be proportionally less (Oke,1992). ψ_s is an important parameter to consider when forecasting RST, due to a two-way influence on the radiation balance.

Firstly, ψ_s has a major impact upon nocturnal cooling rates. Surface geometry causes solar radiation to become trapped in the fabrics of urban canyons. On clear and calm nights, this can result in the urban heat island phenomenon ($T_{(u-r)}$). Oke (1981) studied the relationship between ψ_s and $T_{(u-r)}$ and concluded that heat islands of the order of 8ºC are not impossible as a direct result of canyon geometry and ψ_s.

Secondly, on sunny days, ψ_s acts as a control on the amount of direct solar radiation received at the ground surface. The path of the sun on a particular day is known as a suntrack and is calculated using solar zenith and azimuth angles. If ψ_s is incorporated into the modelling procedure, then buildings will begin to interfere with the solar beam. Hence, there will be some times of the day when a location is not receiving direct solar radiation (though diffuse components will still arrive). Blocking of the solar beam may be so severe, sunset may occur locally far earlier then in surrounding locations, ultimately affecting RST. Therefore, to improve modelling of RST, it is necessary to incorporate ψ_s into the radiation geometry used in 1D climate models.

To date, no definitive technique exists for the calculation of ψ_s with existing techniques having a tendency to be slow. During the eighties, studies into ψ_s were mostly based around geometrical modelling of canyons e.g. Johnson & Watson (1984). Such methods do provide a

rapid appraisal of ψ_s when canyon dimensions are known, but at best they assume 'ideal' canyons with just a couple of elements under consideration. Hence, calculations of ψ_s provided by these approaches are often just estimates. For more accurate results, it is more common to calculate ψ_s from imagery. Figure 1 shows an example of a photograph taken through a fish eye lens showing the sky through 360°, and any intrusions into the clear sky hemisphere such as trees and buildings.

Figure 1 Fish-eye photo of a typical city centre canyon.

Various techniques have been developed to calculate ψ_s from such imagery e.g. Anderson (1964) and Steyn (1980). The main problem is the delineation of sky from buildings and trees in the image. Large variations in image conditions mean that is hard to develop an objective algorithm to do this. Hence, delineation often has to be done by hand which is a very time consuming procedure. If several images need processing, then the calculation of ψ_s becomes a major task. This has ultimately limited research into the climatological impact of ψ_s meaning studies have often had to be confined to incorporate just a few sites. Therefore, to use ψ_s in an energy balance model (EBM), a new calculation approach needed developing.

1. METHODOLOGY

2.1 Calculation of the Sky-View factor

As a result a complete desktop solution to the calculation of ψ_s has been developed using FORTRAN 95. Run entirely in a Windows™ environment. images can now be processed at a rate of around three per second. The main input is a northerly orientated digital greyscale fish-eye photograph (figure 1), ideally taken using a digital camera equipped with a fish-eye lens. Hence, the image can be considered essentially as an array of digital numbers (DN) ranging from 0 to 255.

The problem of delineation again provides the major stumbling block for the calculation of ψ_s, but as we are now dealing with DN the process no longer needs to be carried out by hand. Instead the program uses a critical number thresholding technique which by using a suitable DN, delineates sky pixels from the non-sky pixels in the image. The threshold DN can be easily determined by considering an image histogram (figure 2).

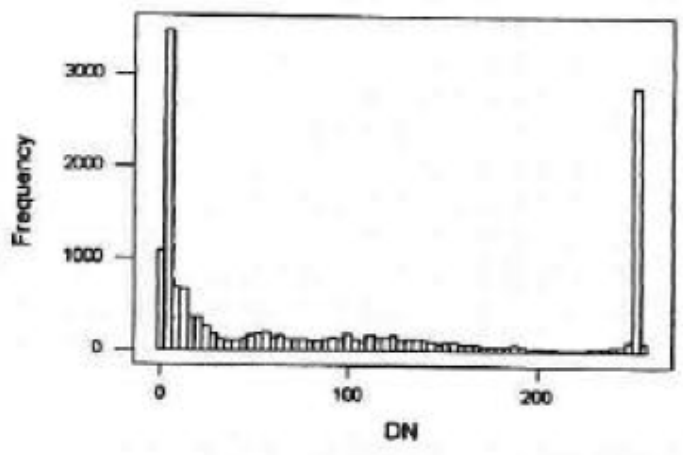

Figure 2 DN histogram of an image taken under ideal conditions

Figure 2 shows the histogram of an image taken in ideal conditions. The distribution is essentially bimodal with a peak of low DN representing the black areas surrounding the fish-eye section of the image and a peak of DN above 250 which represent sky pixels. The plateau of DN in the middle classes represent the buildings in the image. Hence, from this histogram it would be sensible to conclude that a suitable DN for thresholding would be 250. So using a DN of 250, a delineated version of figure one can now be produced (figure 3). The image is now displayed in binary with sky pixels represented as '1'. All other pixels are assigned a '0'.

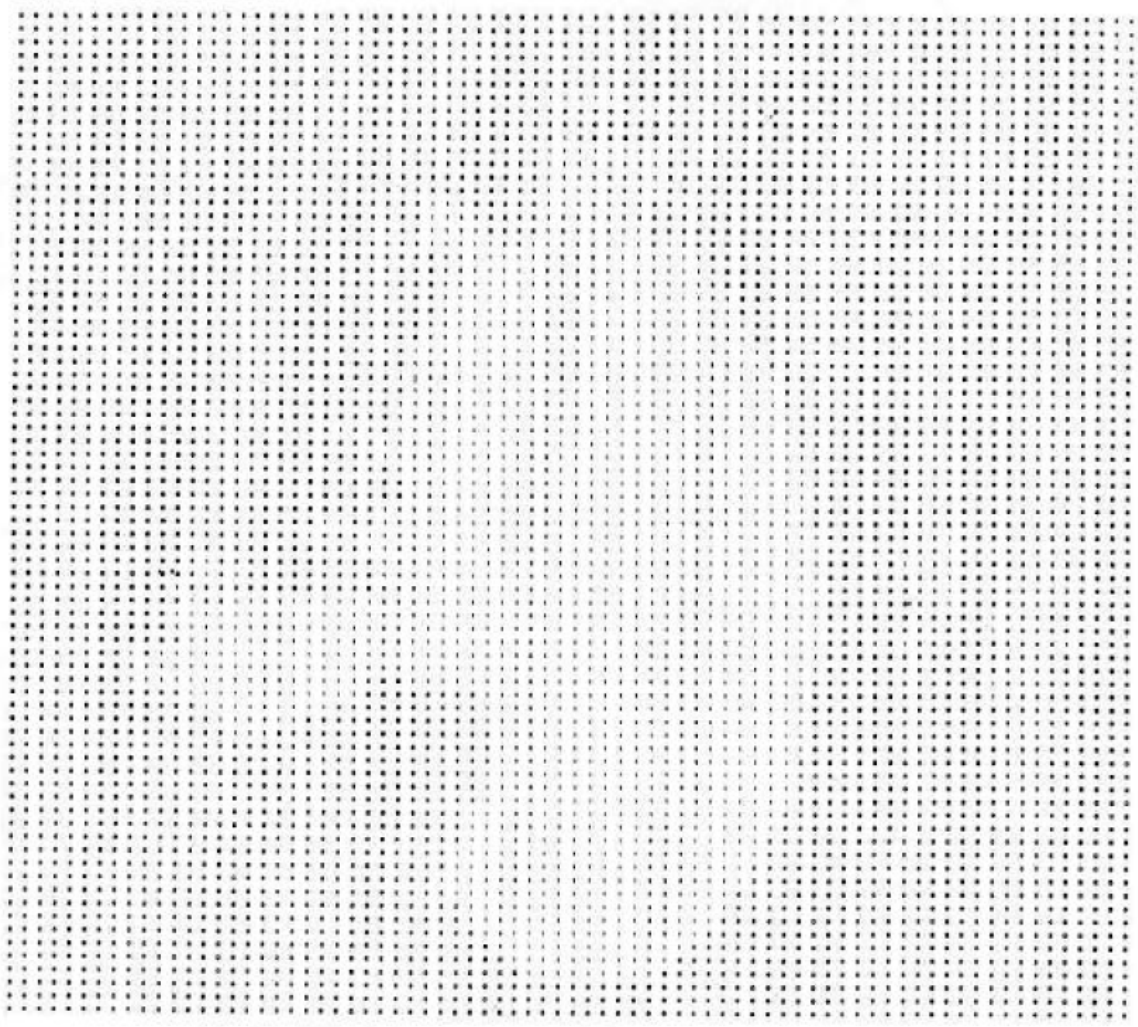

Figure 3 Digitally delineated version of figure one.

Once thresholded, the actual calculation of ψ_s is straightforward and has been developed from the work of Steyn (1980). Steyn delineated the fish eye image into a series of n concentric annuli of equal width and angular width a_i. The sky-view factor is then calculated by:

$$y_s = \frac{1}{2n}\sum_{i=1}\sin\left(\frac{p\,(i-0.5)}{2n}\right)\cos\left(\frac{p\,(i-0.5)}{2n}\right)a_i \qquad (1)$$

Where i is the annuli number. By the use of a template the thresholded image can also be assessed as a series of concentric annuli. Then by calculating the percentage of sky pixels in each annulus to the total number of pixels per annulus on the template, an approximation for a_i be obtained. Equation one now reads as:

$$y_s = \frac{1}{4n}\sum_{i=1}\left(\sin\frac{p\,(2i-1)}{2n}\right)\left(\frac{p_i}{t_i}2p\right) \qquad (2)$$

Where p_i is the number of pixels corresponding to those marked i on the template and t_i is the total number of pixels in the ith annulus.

2.1 Estimation of Suntrack Intrusion

In order to investigate how surrounding trees and buildings will impact upon the sky hemisphere and hence the suntrack, it is necessary to have an understanding of how surrounding objects are projected onto a fish eye photograph. The projection of an object onto a fisheye image is shown in figure 4. Steyn (1980) showed that the actual protrusion of an object onto the image can be by calculated simply by considering the building angle (ζ).

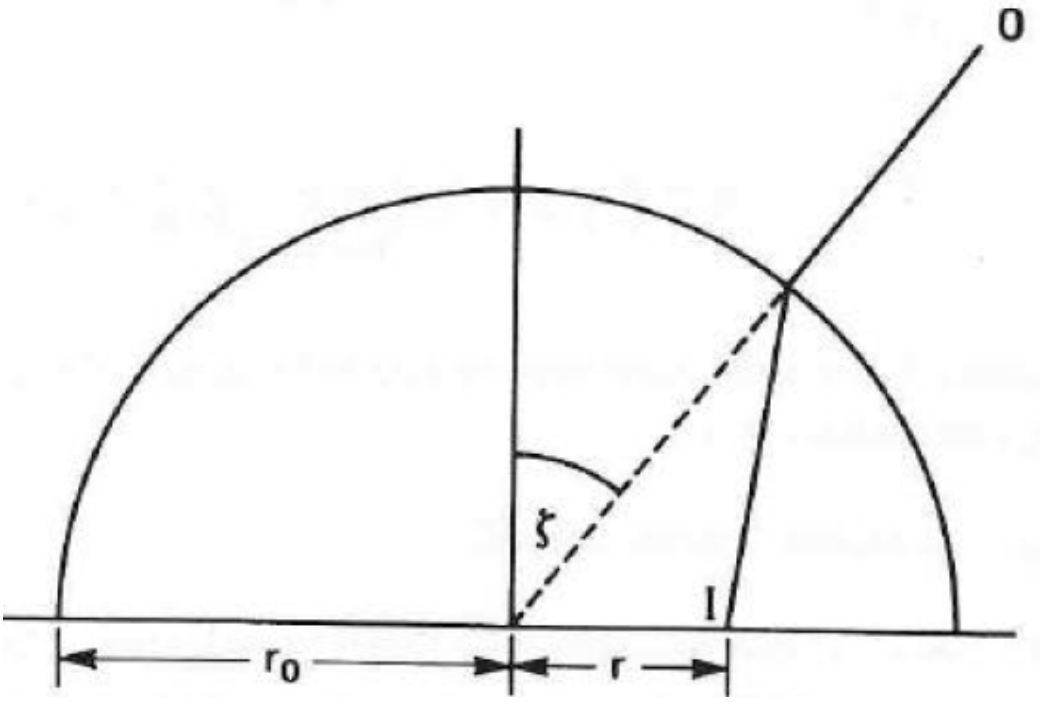

Figure 4 Fisheye lens projection where O is the object and I is the *image (Steyn, 1980).*

The implications of this is that as the length of protrusion of an object can be measured off a fisheye image, it is then possible to calculate ζ between the site where the image was taken and the top of the object. Hence, for anytime of the day ζ can be compared with the solar zenith and azimuth angles to determine whether the site will be receiving direct beam radiation.

Figure 5 shows how the angle of the solar beam varies with ζ for the image shown in figure 1. The solar angle never actually gets above 30 degrees at this time of year, and hence, buildings obscure the sun for long periods. Direct solar beam is only actually received for about 45 minutes in the morning and up to around 2pm. After this time, the only contribution to the radiation balance will be diffuse radiation.

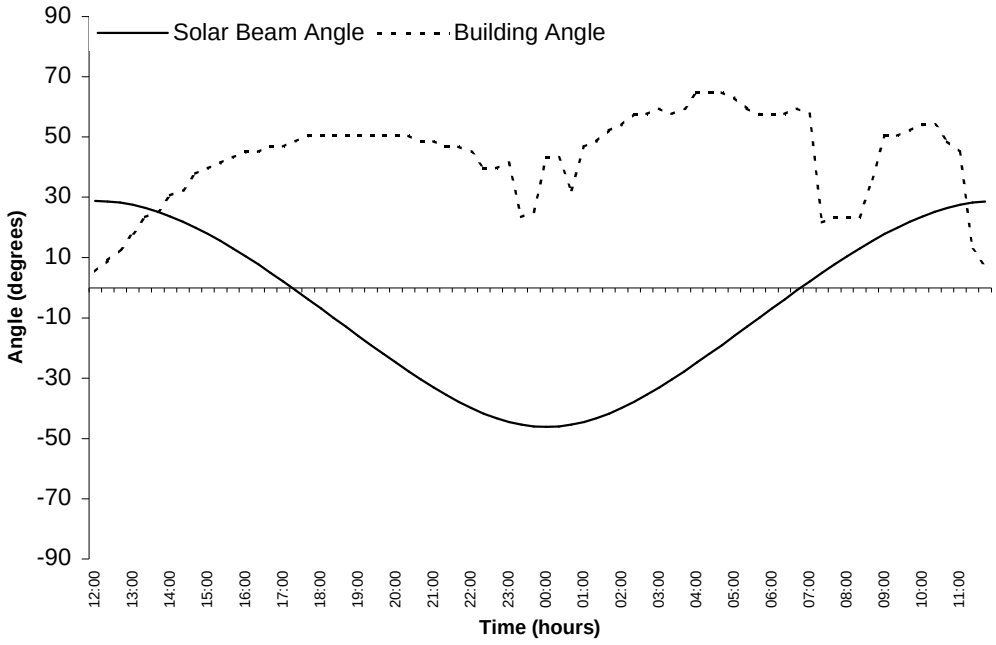

Figure 5 Plot of building and solar beam angles for figure 1 over a 24 hour period. (Julian Day=59, Latitude=52.5)

2.3 Incorporation into a 1D EBM

The sky-view calculation program was included as a subroutine in Thornes (1984) 1D EBM road weather prediction model. To include ψ_s in the modelling of the long-wave flux of the EBM, ψ_s is simply inserted as an extra coefficient in the Stefan Boltzmann equation:

$$E = e s y_s T^4 \tag{3}$$

Secondly, the impact of ψ_s on the short wave flux was incorporated into the model by calculating ζ and the angle of the solar beam every twenty minutes. The direct beam component of the balance is then switched off whenever ζ exceeds the angle of the direct solar beam.

3 RESULTS & DISCUSSION

The techniques described in this paper are currently in their infancy, hence the only results available at the time of press are of the form of sensitivity tests. Figure 6 shows a series of forecast curves generated by the model using the same climate data for a variety of locations with differing ψ_s.

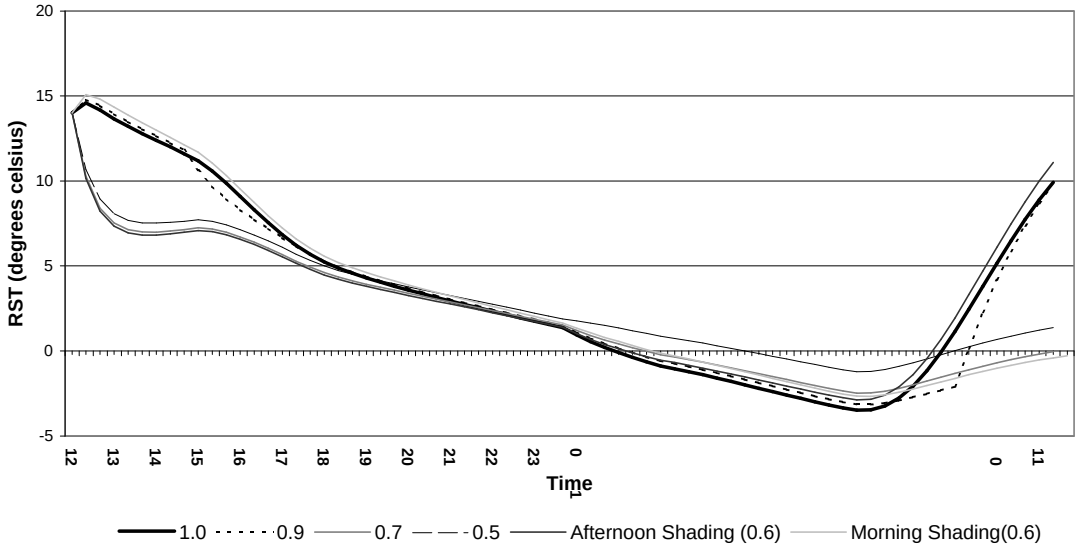

Figure 6 Sensitivity test of Thornes (1984) road-weather prediction model incorporating sky-view factor analysis. The same hypothetical data is used for a variety of sky-view factors.

Figure 6 shows that the impact of ψ_s on RST can be very important. From the point of view of winter road maintenance, a simple rule of thumb appears to be that as ψ_s approaches unity, RST will become subsequently lower. This is a direct result of increased long-wave radiation losses found in open terrain. Hence, it would be sensible to conclude that during marginal nights (nights where RST hovers around the 0ºC threshold) only roads with a high sky-view need be treated.

However, the situation is not that simple and the impact of ψ_s on incoming solar also needs considering. Figure 6 shows that the site with afternoon shading is up to around 7°C colder during the day than sites with an open sky-view. This disparity between sites continues throughout the forecast (though at a much smaller magnitude) causing RST's at these sites to be slightly lower throughout the night. A phenomenon also recognised by Karlsson (1999), meaning that sites with a lower sky-view may actually have a lower RST. Similarly, sites

with morning shading remain much colder after sunrise as no direct beam radiation can reach the road surface. This disparity in heating rates between sites can result in the lesser documented phenomena of the urban cold island where urban areas are actually colder then surrounding rural areas.

4 CONCLUSIONS

A technique has been described which allows rapid calculation of the ψ_s and associated corrected suntrack from a digital image. Provided care is taken in the early stages of image processing and subsequent thresholding, the results obtained will be accurate and suitable for use in climatological modelling. The rapid nature of the process allows the fast processing of many images at speed, enabling climatological modelling including ψ_s to be developed on a scale not previously possible.

It has been shown that ψ_s has a considerable influence on RST and as a parameter could be used as a surrogate to thermal mapping techniques. The implications of this for winter road maintenance is that instead of a single forecast curve being produced and extrapolated by means of a thermal map, it may be possible to produce a different forecast curve for each section of a road network. This could be achieved quickly by simply varying ψ_s and other geographical parameters such as altitude and latitude in a 1D EBM.

5. REFERENCES

A**nderson, M.C. (1964)** Studies of woodland light climate. *Journal of Applied ecology* **52** pp27-41

Johnson, G.T. & Watson, I.D. (1984) The determination of view-factors in urban canyons. *Journal of Applied Climate and Meteorology* **23**. pp329-335

Karlsson (1999) Local and micro climatological studies with emphasis on temperature variations and road slipperiness. *Unpublished PhD Thesis*. University of Gothenberg

Oke, T.R. (1992) *Boundary Layer Climates* . Routledge pp232,237,286,288,293-294.

Steyn, D.G. (1980) The calculation of view-factors from fisheye-lens photographs: Research Note. *Journal of Atmospheric and Ocean Sciences* **18.3** pp254-258

Thornes, J.E. (1984) The prediction of ice formation on motorways in Britain *Unpublished PhD Thesis.* University of London